Development, Fabrication and Characterization of Lumped Element Kinetic Inductance Detectors for NIKA

M. Roesch[1,*], L. Swenson[2], A. Bideaud[2], A.Benoit[2], S. Doyle[3], K.F. Schuster[1] and A. Monfardini[2] for the NIKA collaboration
[1]*IRAM, Institut de Radioastronomie Millimétrique, St. Martin d'Hères, France*
[2]*Institut NEEL, Grenoble, France*
[3]*Department of Physics and Astronomy, Cardiff, CF243AA*
*Contact: roesch@iram.fr

***Abstract*— Lumped-element kinetic inductance detectors (LEKIDs) have recently shown considerable promise as direct-absorption mm-wavelength detectors for astronomical applications. One major research thrust within the Néel Iram Kids Array (NIKA) collaboration has been to investigate the suitability of these detectors for deployment at the 30-meter IRAM telescope located on Pico Veleta in Spain. In order to optimize the LEKIDs for this application, we have recently probed a wide variety of individual resonator and array parameters through simulation and physical testing. This included determining the optimal feed-line coupling, pixel geometry, resonator distribution within an array (in order to minimize pixel cross-talk), and resonator frequency spacing. Based on these results, a 32-pixel Aluminum array was fabricated and tested in a dilution fridge with optical access, yielding an average optical NEP of ~1 x 10-15 W/Hz^1/2.**

I. Introduction

Since 2003 kinetic inductance detectors (KID) are considered as promising alternative to classical bolometer for mm and sub-mm astronomy [2]. Photons, with energy higher than the gap energy ($E=h\cdot v>2\Delta$), break cooper pairs in a superconducting film. This leads to an increase in number of quasi particles, which changes the surface reactance of the superconductor (kinetic inductance effect) [6].

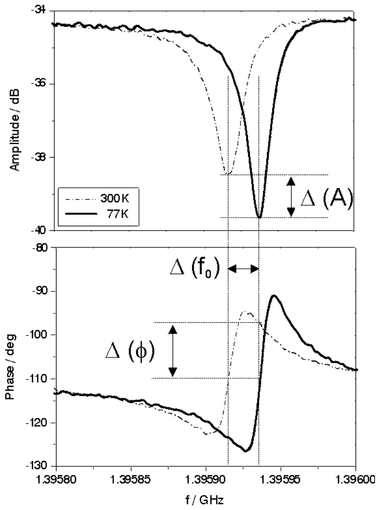

Fig. 2 Principle of KIDs. Solid lines: under dark conditions; dashed line: optical load of 300 K.

One possibility to make advantage of this effect is to use a superconducting resonant circuit as detecting element. A measurement of such a resonator coupled to a transmission line is shown in Fig. 1. An illumination of he detector leads to a shift in resonance frequency f_0, which can be measured through a change in amplitude and phase. One advantage of KIDs is the easy fabrication process. Due to only one metallisation layer on a substrate, it is less complicated compared to bolometer fabrication. Another advantage of KIDs resides in the readout system. Frequency multiplexing allows the readout of a large number of resonators. Packed in a limited bandwidth, a single transmission line is sufficient to read out several hundreds of pixel.

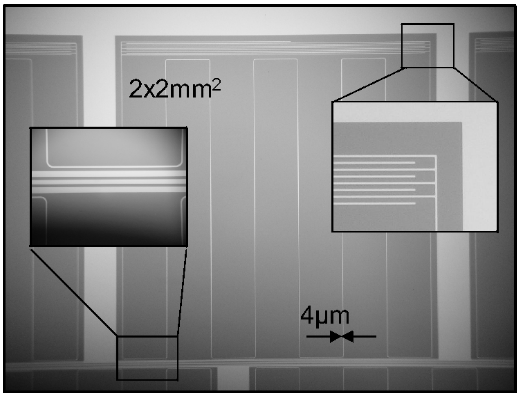

Fig. 1 LEKID geometry. Enlarged left hand side: coupling area; right hand side: interdigital capacitor.

In Fig 2, one resonator design, a so-called lumped element kinetic inductance detector (LEKID) is shown. Simon Doyle first proposed this type of resonator in 2008 [1]. Compared to other microwave resonators (quarter wavelength resonator [3]), this type consists of a long meandered line, the inductive part, and an interdigital capacitor. A very high and constant current density over the whole length of the meander makes this part a very sensitive direct detection area. The optical efficiency can be optimised by changing the geometry of the meander. Therefore, there are no lenses or antenna structures necessary to couple the incoming microwaves into the resonator.

The NEEL IRAM KIDs array (NIKA) is a collaboration of several groups to develop a multi pixel camera based on kinetic inductance detectors for the IRAM 30m telescope located in Spain [4]. Here we present the development of a LEKID array for NIKA. Measurement results of electrical (coupling, frequency distribution) and optical characterization (optical coupling, NEP) are presented in this paper.

II. CHARACTERIZATION OF LEKIDS

A. *Electrical characterization*

To test parameters like coupling strength and frequency tuning, several test arrays were designed. In Fig. 3 one of the 6-pixels test chip is shown. The samples were fabricated with a 60 nm Nb film that on top of a high resistance (>5kOhms) silicon substrate. The critical temperature of Nb (Tc=9.2K) allows measuring the samples in liquid Helium (T=4.2K). Due to a pumping system, connected to the cryostat, a minimum temperature of 2 K was reached for the measurements of the Nb-samples.

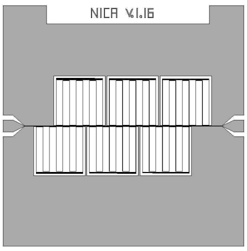

Fig. 3 Layout of a 6-pixel LEKID array for the el. characterization.

To investigate the coupling of a LEKID to a transmission line we varied the width of the ground plane between the transmissions line and the meander (see Fig. 2). In Fig. 4 the measurement curves of two resonators with different couplings are shown. The resonance dip of the solid line is much deeper, due to a stronger coupling. The intrinsic quality factor, Q_0, was calculated to be 10^5 for the 60 nm Nb film @ 2K. The coupling quality factor for the less coupled resonator was determined to be ~150 000, for the stronger coupled ~80 000.

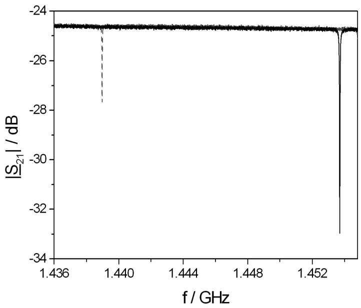

Fig. 4 Measurements of two LEKID arrays with different couplings (one resonator of each array). Dashed line: 20 µm ground plane; solid line: 10 µm ground plane.

Another important factor, in order to pack as many resonators as possible in a limited bandwidth, is the frequency spacing between the resonances. Therefore, it is necessary to be able to simulate the frequency tuning before making the design for a big array to avoid overlapping resonances. The simulations [8] showed a non-linearity in frequency tuning when the number of fingers of the capacitor is too low. In Fig. 5 the comparison of simulation and measurement is shown for two different arrays.

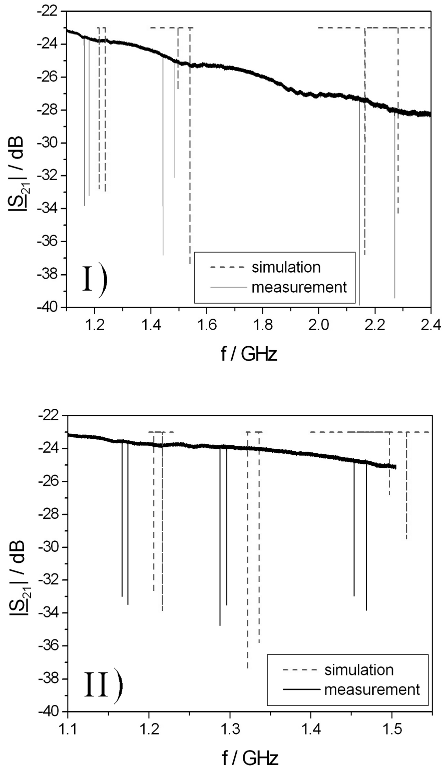

Fig. 5 Comparison of simulation (dashed lines)[8] and measurement (solid lines) to investigate the frequency tuning by changing the number and length of the capacitor fingers. I) bandwidth ~1 Ghz; II) bandwidth: ~300 Mhz.

The resonances of sample (I) are distributed in a bandwidth of ~1 Ghz. For the second array (II) a bandwidth of ~300 Mhz was chosen. A shift of the simulated resonances to higher frequencies is due to the value of the kinetic inductance (Ls) in sonnet. In I), the highest two resonance frequencies are less shifted compared to the others, the reason for that is the limited bandwidth of the amplifier. Beside these explainable shifts, Fig. 5 shows a good agreement between simulation and measurement. Further is there a number of fingers that should not be decreased in order to avoid a shift of the resonances to much higher frequencies. In this case the number of fingers of the capacitor was varied from three to nine. In between, the length of the fingers was varied as well.

B. *Optical characterization*

Based on the measurement of the Nb test array, a 32-pixels array was designed for optical characterization of the LEKIDs. The arrays were fabricated and tested in a dilution fridge with optical access. They were made with an aluminium film (Tc=1.2K) on a high resistance (>5kOhms) silicon substrate. Two different arrays were fabricated, one with a metallization thickness of 40 nm, the second one with 60 nm thick film. A schematic of the optical measurement setup is shown in Fig. 6. On a XY-table, a so-called sky simulator is placed. It consists of a mirror (A), a chopper (B) and a box filled with liquid nitrogen (D). In the box there is an absorber material (C) with a hole of 1 cm in diameter in the centre. This configuration was built to be as close as possible to the background conditions at the telescope. The cryostat itself is a ^{3}He-^{4}He-dilution fridge with a minimum temperature of T=100 mK. Between the focal plane (F), where the array is mounted, and the optical access, there are several filters allowing to cut the IR load and to define the bandwidth of 125-170 GHz.

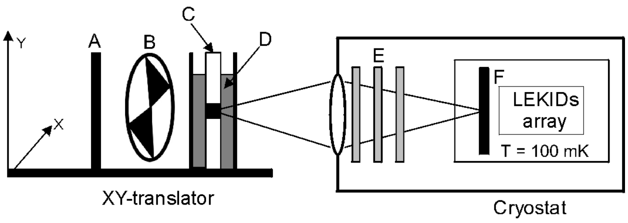

Fig. 6 Configuration of the cryostat and the XY-translator. A) Mirror, B) Chopper, C) Absorber with a hole of 1 cm of diameter, D) Liquid nitrogen, E) Optical filters for a bandwidth from 125 to 170 GHz, F) LEKID array in the focal plane at the 100 mK stage.

In Fig. 7 a schematic of the measurement configuration, including the readout electronics [5], [7], is shown. The frequencies are digitally created in the FPGA in a limited bandwidth of 45 MHz before they are DA-converted. To excite the resonators the frequencies are up-converted to the actual resonance frequencies using an IQ-mixer (C) and a synthesizer (A). After the signal has passed the cryostat, it is amplified (E) at 4K and at room temperature. To readout the signal, it has to be down-converted (C) to the original bandwidth of the FPGA. In the FPGA a Fast Fourrier transformation is done to separate each resonator signal.

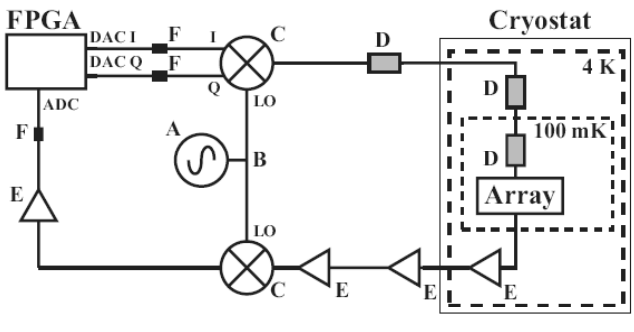

Fig. 7 Basic measurement schematic: A) High-frequency synthesizer, B) Splitter, C) IQ-Mixer, D) Attenuator, E) Amplifier and F) Low-pass filter.

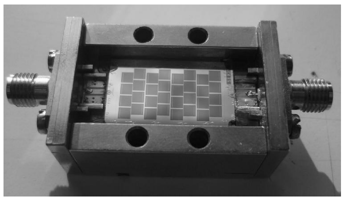

Fig. 8 Mounted 32-pixel array in a gold plated copper sample holder.

Fig. 8 shows the 32-pixel array mounted in a gold plated copper sample holder. To optimize the optical absorption, a back-short cavity was mounted in a calculated distance, d = lambda$_{eff}$/4, to the array. To check the distribution of the resonances, a frequency scan was done, as shown in Fig. 9. Due to fabrication errors and parasitic magnetic fields, the resonances are not equally spaced. For this array 30 out of 32 resonators worked. We calculated an average intrinsic quality factor of $Q_0 \approx 10^5$ and a loaded quality factor of $Q_L \approx 50\,000$. After we did an optical scan, using the XY-table and the chopper, over the whole area of the array to determine the location of each pixel. During the scan, the phase response of each pixel changes, depending on the position of the table.

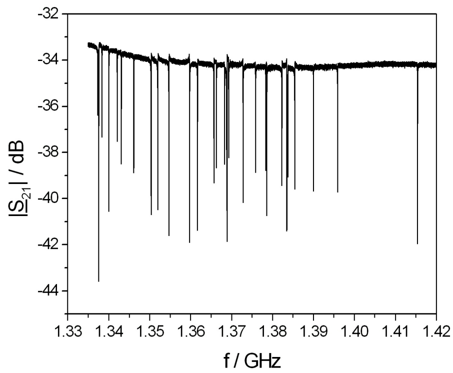

Fig. 9 Frequency scan (S21) over all resonance frequencies of the array.

In Fig. 10 the location of the maximum response of each pixel is plotted over the fabricated array. This beam pattern shows a good agreement in pixel distribution compared to the real array. Double resonances can cause calculation errors in the FPGA, leading to a wrong location of the pixel in the XY-plane (as seen in Fig 10).

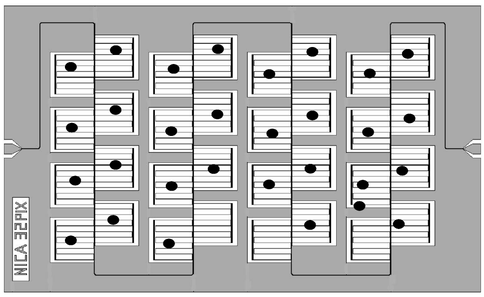

Fig. 10 Beam pattern of the 32-pixel LEKID array. Dots: Position of maximum optical response of each pixel

The spectrum of the phase noise of the array is shown in Fig. 11. The roll-off above 30 Hz is related to the read-out electronics rate. We calculated an average detector phase noise at 1 Hz of 5 mdeg/Hz$^{1/2}$. With an average phase signal of 5 degree and

$$NEP = \frac{P}{S/N}\frac{1}{\sqrt{\tau}},$$

the optical Noise Equivalent Power (NEP) was determined to be around 1×10^{-15} W/Hz$^{1/2}$for the 40 nm thick film. With P the optical power on one pixel, the signal to noise ratio S/N and the integration time τ of the Fourrier transformation. We gained a factor of 2 in NEP by reducing the film thickness from 60 nm to 40 nm. The kinetic inductance in the meander line increases due to a smaller volume of the line. A higher kinetic induction fraction α leads to a higher sensitivity.

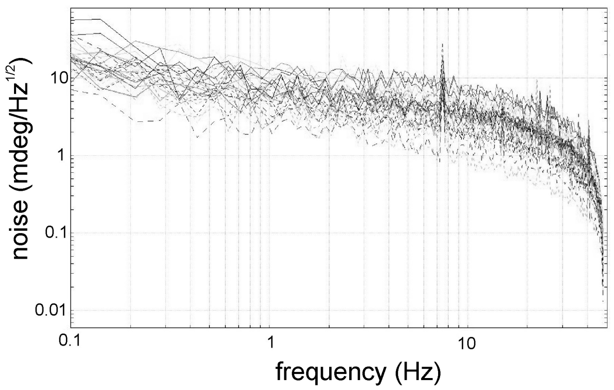

Fig. 11 Spectrum of the phase noise of each pixel without the chopper.

III. Conclusions

The promising measurement results presented in this paper show a high potential of the LEKIDs for mm and sub-mm detection. The easy fabrication and the Frequency-Multiplexing make them feasible for developing arrays with several hundreds of pixels. The good agreement between simulations and measurements makes it possible to simulate the design of a much bigger array.

In October 2009 a 30-pixel LEKID array was tested at the IRAM 30 m telescope in Spain and achieved first astronomical results [4].

References

[1] S. Doyle, “Lumped Element Kinetic Inductance Detectors,” thesis, Cardiff University, Cardiff, Wales, April. 2008.

[2] P.K. Day, H.G. LeDuc, B.A. Mazin, A. Vayonakis and J. Zmuidzinas, “A broadband superconducting detector suitable for use in large arrays,” *Nature*, 425, 817, 2003.

[3] B.A. Mazin, “Microwave Kinetic Inductance Detectors,” thesis, California Institute of Tecnology, Pasadena, California, USA, 2004.

[4] A. Monfardini, et al. NIKA: A Millimeter-Wave Kinetic Inductance Camera, Astronomy & Astrophysics, 2010, to be submitted.

[5] L.J. Swenson, J.. Minet, G.J. Grabovskij, et al., in AIP Proc., 2009, paper 1185, p. 84.

[6] M. Tinkham, Introduction to Superconductivity, Krieger Pub Co, 1975.

[7] S.J.C. Yates, J.J.A. Baselmans, A.M. Baryshev, et al., in AIP Proc., 2009, paper 1185, p. 249.

[8] “Sonnet User’s Guide-Manual of the Program Sonnet,” Sonnet Software, Inc., 2007, 100 Elwood Davis Road, North Syracuse, NY13212, USA.